# APPLICATION OF REPRODUCING KERNEL ALGORITHM FOR SINGULAR BVPs INVOLVING FREDHOLM-VOLTERRA OPERATOR

**Asad Freihat**
*Department of Applied Science*
*Ajloun College*
*Al-Balqa Applied University*
*Ajloun 26816, Jordan*
*asadfreihat@bau.edu.jo*

**Abstract.** This paper proposes asymptotically efficient algorithm for treating classes of singular boundary value problems involving Fredholm and Volterra operators associated with three-point boundary conditions. The algorithm methodology is proposed based on the novel reproducing kernel Hilbert space (RKHS) method, which is used directly without employing linearization and perturbation. The orthonormal system is generated in a favorable Hilbert space on a compact dense interval to expand the solution in Fourier series formula with accurately computable components. Numerical examples of singular multipoint BVPs are performed to support the theoretical statements that acquired by interrupting the $n$-term of the exact solutions. Besides, the results obtained indicate that the RK procedure is effective and competitive with a great capability in scientific and engineering applications.

**Keywords:** singular boundary value problems, Fredholm and Volterra operators, reproducing kernel Hilbert space method.

## 1 Introduction

Singular boundary value problems associated with three-point boundary conditions have been investigated in a wide area of mathematics, physics and engineering including dynamics, nuclear, chemical reaction, atomic structures and so on [1, 2, 3, 4]. Indeed, the scientific issues in this area often occur to be nonlinear with a finite set of singularity, which they are very difficult to be handled analytically through classical way. In this situation, solutions needed could not be accurately determined or fail to be convergent due to singularity. So, it has to be solved using advanced numerical and computational methods. Unfortunately, these methods are very limited unless we can resort to linearization and discretization of the variables to deal with them. Thus, it appears to be very important to develop an efficient numerical method for handling such problems. Anyhow, some numerical approaches for solving second-order, singular three point boundary value problems (BVPs) are available in literature [3, 4, 5, 6, 7]. But, there is a few research papers about second-order, singular three-point BVPs restricted by Fredholm or Volterra operators.

The purpose of this study is to investigate and implement a computational iterative technique, the reproducing kernel Hilbert space method (RKHS), in finding approximate solutions for a certain class of singular BVPs. More specifically, we consider second order three-point singular BVP in the following differential operator form:

$$u''(t)+\frac{a(t)}{p(t)}u'(t)+\frac{b(t)}{q(t)}u(t)=f(t,u(t),Tu(t)),0\leq t\leq 1, \tag{1}$$

associated with three-point boundary conditions

$$u(0)=0,\ u(1)=\alpha u(\eta),\ 0<\eta<1,\ \alpha>0,\ \alpha\eta<1, \tag{2}$$

where $a(t),b(t)\in C^2(0,1)$,

$$Tu(t)=\lambda_1\int_0^1 h_1(t,s)\,G_1(u(s))\,ds+\lambda_2\int_0^t h_2(t,s)\,G_2(u(s))\,ds,\lambda_i,i=1,2,$$

are positive parameters, $h_i(t,s),i=1,2$, are arbitrary analytical kernel functions over the square $0<s<t<1$, $G_1(v_1),G_2(v_2)$ are linear or nonlinear continuous terms in $\Pi_1[0,1]$ as $v_i=v_i(t)\in\Pi_3[0,1]$, $0\leq t\leq 1$, $-\infty<v_i<\infty$, $i=1,2$, $f(t,u,Tu)\in\Pi_1[0,1]$ are sufficiently regular given functions such that singular BVPs (1) and (2) satisfies the existence and uniqueness of the solutions, and $u\in\Pi_3[0,1]$ is an unknown function to be determined. Here, the real-valued functions $p(t)$ and $q(t)$ are continuous and may be equal to zero at $\{t_i\}_{i=1}^m\in[0,1]$; that is, the equation may be singular at $t=t_i,i=1,2,...,m$.

The reproducing-kernel is a numerical as well as analytical algorithm for treating a wide variety of ODEs and PDEs associated to different kinds of order derivatives degree, which usually provides the solutions in terms of rapidly convergent series with components that can be elegantly computed [8, 9, 10, 11, 12]. The RKHS algorithm has been successfully applied to various areas in numerical analysis, computational mathematics, image processing, machine learning, quantum mechanics, and finance [13, 14, 15, 16] Moreover, in the recent years, a lot of research work has been devoted to utilize the RKHS method as a superb framework to find numerical approximate solutions to diverse matters [17, 18, 19, 20, 21, 22, 23]. On the other hand as well, the numerical solvability of different categories of BVPs can be found in [24, 25, 26, 27, 28, 29, 30].

The objective of this article is to highlight the importance of singular BVPs in sobolev spaces for specific applications. The structure of this article is organized as follows: In the next section, necessary details and preliminaries about the reproducing-kernel theory are briefly given. In section 3, theoretical and analytical basis with representation of solutions are introduced in the Hilbert space $\Pi_3[0,1]$. Convergence analysis of the method are presented in section 4 Numerical outcomes are investigated in section 5. A final section provides brief conclusions.

## 2 Background and preliminaries

In this section, we present the concept of essential materials about the RKHS method for constructing smooth reproducing-kernel functions which will used to produce a set of orthonormal basis functions, as well as, derive the solutions in terms of Fourier series coefficients in Sobolev spaces. To do that, multiply both sides of Eq. (1) by $p(t)\,q(t)$ to get

$$\widetilde{P}(t)\,u''(t)+\widetilde{Q}(t)\,u'(t)+\widetilde{R}(t)\,u(t)=\widetilde{F}(t,u(t),Tu(t)), \tag{3}$$

where $\widetilde{P}(t)=p(t)\,q(t)$, $\widetilde{Q}(t)=a(t)\,q(t)$, $\widetilde{R}(t)=b(t)\,p(t)$, and $\widetilde{F}(t,u,Tu)=p(t)\,q(t)\,f(t,u,Tu)$.

If we defined a function $v(t)=u(t)-\gamma t$, $\gamma=\alpha u(\eta)$, then Eq. (3) can be reduced to the following form:

$$\widetilde{P}(t)\,v''(t)+\widetilde{Q}(t)\,v'(t)+\widetilde{R}(t)\,v(t)=\widetilde{G}(t,v(t),Tv(t)), \tag{4}$$

with the homogeneous boundary conditions

$$v(0)=0,\ v(1)=0, \tag{5}$$

where $\widetilde{G}(t,v(t),Tv(t))=\widetilde{F}(t,u(t)+\gamma t,T(u(t)+\gamma t))-\gamma(t\widetilde{R}(t)+\widetilde{Q}(t))$. Obviously, it suffices for us to solve BVPs (4) and (5).

**Definition 1** ([11]). *Let $\mathcal{H}$ be a Hilbert space of function $\mathcal{F}:\Omega\to\mathcal{H}$ on a set $\Omega$. A function $\Gamma:\Omega\times\Omega\to\mathbb{R}$ is a reproducing kernel of $\mathcal{H}$ if the following conditions are satisfied: Firstly, $\Gamma(\cdot,s)\in\mathcal{H}$ for each $s\in\Omega$. Secondly, $\langle\mathcal{F}(\cdot),\Gamma(\cdot,s)\rangle=\mathcal{F}(s)$ for each $\mathcal{F}\in\mathcal{H}$ and each $s\in\Omega$.*

**Definition 2** ([8]). *The space $\Pi_1[0,1]$ is defined as $\Pi_1[0,1]=\{v=v(t):v$ is one-variable absolutely continuous real-valued function on $[0,1]$ and $v'\in L^2[0,1]\}$. Whilst, the inner product and the norm of $\Pi_1[0,1]$ are given, respectively, by*

$$\langle v_1(t),v_2(t)\rangle_{\Pi_1}=v_1(0)\,v_2(0)+\int_0^1 v_1'(s)v_2'(s)ds, \tag{6}$$

*and $||v_1(t)||^2_{\Pi_1}=\langle v_1(t),v_1(t)\rangle_{\Pi_1}$, where $v_1,v_2\in\Pi_1[0,1]$.*

**Theorem 3** ([8]). *The Hilbert space $\Pi_1[0,1]$ is a complete reproducing kernel with the reproducing kernel function*

$$\widehat{G}_s(t)=\begin{cases}1+t, & t\le s,\\ 1+s, & t>s.\end{cases} \tag{7}$$

Now, we construct the reproducing kernel space $\Pi_3[0,1]$ in which every function satisfies the boundary conditions $v(0)=0$ and $v(1)=0$.

**Definition 4.** *The space* $\Pi_3[0,1]$ *is defined as* $\Pi_3[0,1] = \{v = v(t) : v, v', v''$ *are one-variable absolutely continuous real-valued functions on* $[0,1]$, $v''' \in L^2[0,1]$, *and* $v(0) = 0, v(1) = 0\}$. *Whilst, the inner product and the norm of* $\Pi_3[0,1]$ *are given, respectively, by*

$$\langle v_1(t), v_2(t)\rangle_{\Pi_3} = \sum_{i=0}^{1} v_1^{(i)}(0)\, v_2^{(i)}(0) + v_1(1)v_2(1) + \int_0^1 v_1'''(w)v_2'''(w)dw, \tag{8}$$

*and* $||v_1(t)||^2_{\Pi_3} = \langle v_1(t), v_1(t)\rangle_{\Pi_3}$, *where* $v_1, v_2 \in \Pi_3[0,1]$.

**Theorem 5.** *The Hilbert space* $\Pi_3[0,1]$ *is a complete reproducing kernel with reproducing kernel function*

$$G_s(t) = \begin{cases} \frac{1}{120}(1-t)^3 s^3\left[6s^2t^2 + 3st(s-5t) + (10t^2 - 5st + s^2)\right], & t \le s, \\ \frac{1}{120}(1-s)^3 t^3\left[6s^2t^2 + 3st(t-5s) + (10s^2 - 5st + t^2)\right], & t > s. \end{cases} \tag{9}$$

**Proof.** According to [8], $\Pi_3[0,1]$ is a complete reproducing kernel Hilbert space, that is, for each fixed $s \in [0,1]$ and any $v(t) \in \Pi_3[0,1]$, there exists a function $G_s(t) \in \Pi_3[0,1]$ such that $\langle v(s), G_t(s)\rangle_{\Pi_3} = v(t)$, $t \in [0,1]$ and the expression form of $G_s(t)$ can be denoted as $G_s(t) = \sum_{i=1}^{6} a_i(s)t^{i-1}$, if $t \le s$, and $G_s(t) = \sum_{i=1}^{6} b_i(s)t^{i-1}$, if $t > s$, where the coefficients $a_i(s)$ and $b_i(s)$, $i = 1, 2, ..., 6$, could be obtained by solving the following generalized differential equations using Maple 13 software package:

$$\begin{array}{l} G_s(0) = 0, \partial_t G_s(0) + \partial_t^4 G_s(0) = 0, \partial_t^3 G_s(0) = 0, \\ G_s(1) = 1, \partial_t^i G_s(1) = 0, i = 3, 4, \\ \partial_t^6 G_s(t) = -\delta(s-t),\ \delta \text{ dirac-delta function}, \\ \partial_t^i G_s(s-0) = \partial_t^i G_s(s+0), i = 0, 1, ..., 4, \\ \partial_t^5 G_s(s+0) - \partial_t^5 G_s(s-0) = -1. \end{array} \tag{10}$$

The proof is complete. □

## 3 Theoretical and analytical basis

In order to illustrate the RKHS methodology to proposed model, we consider that $\mathcal{D} : \Pi_3[0,1] \to \Pi_1[0,1]$ is an invertible bounded linear operator such that $\mathcal{D}v(t) := \widetilde{P}(t)\, v''(t) + \widetilde{Q}(t)\, v'(t) + \widetilde{R}(t)\, v(t)$, and $\mathcal{D}^*$ is the adjoint operator of $\mathcal{D}$. Then, Eqs. (4) and (5) can be equivalently converted into the form:

$$\begin{cases} \mathcal{D}v(t) = \widetilde{G}(t, v(t), Tv(t)), \\ v(0) = 0, v(1) = 0. \end{cases} \tag{11}$$

Let $\varphi_i(t) = G_{t_i}(t)$ and $\psi_i(t) = \mathcal{D}^*\varphi_i(t)$, where $\{t_i\}_{i=1}^{\infty}$ is a countable dense subset in $[0,1]$. From the reproducing-kernel property, it holds $\langle v(t), \varphi_i(t)\rangle_{\Pi_1} = v(t_i)$.

**Theorem 6.** *Suppose that* $\{t_i\}_{i=1}^{\infty}$ *is dense in the interval* $[0,1]$*, then the sequence* $\{\psi_i(t)\}_{i=1}^{\infty}$ *is a complete function system in* $\Pi_3[0,1]$ *with* $\psi_i(t) = .(\widetilde{P}(s)\partial_s^2 + \widetilde{Q}(s)\partial_s + \widetilde{R}(s))[G_t(s)]|_{s=t_i}$.

**Proof.** In this proof, the subscript $s$ by the operator $\mathcal{D}$, denoted by $\mathcal{D}_s$, indicates that the operator $\mathcal{D}$ applies to the function of $s$. However, it is clear that $\psi_i(t) = \mathcal{D}^*\varphi_i(t) = \langle \mathcal{D}^*\varphi_i(t), G_t(s)\rangle_{\Pi_3} = \langle \varphi_i(t), \mathcal{D}_s G_t(s)\rangle_{\Pi_1} = .\mathcal{D}_s G_t(s)|_{s=t_i} = .(\widetilde{P}(s)\partial_s^2 + \widetilde{Q}(s)\partial_s + \widetilde{R}(s))[G_t(s)]|_{s=t_i}$.

Since $\{t_i\}_{i=1}^{\infty}$ is dense in the interval $[0,1]$. For each $v(t)$ in $\Pi_3[0,1]$, if $\langle v(t), \psi_i(t)\rangle_{\Pi_3} = \langle \mathcal{D}v(t), \varphi_i(t)\rangle_{\Pi_1} = \mathcal{D}v(t_i) = 0$, $(i = 1, 2, ...)$, then from the density of $\{t_i\}_{i=1}^{\infty}$ and continuity of $v(t)$, we have $v(t) = 0$. □

The RKHS solution will be obtained by calculating a truncated series based on the orthonormal functions $\{\overline{\psi}_i(t)\}_{i=1}^{\infty}$ of the space $\Pi_3[0,1]$, which is constructed from $\{\psi_i(t)\}_{i=1}^{\infty}$ by using the Gram-Schmidt process such that

$$\bar{\psi}_i(t) = \sum_{k=1}^{i} \mu_{ik}\psi_k(t), \ (\mu_{ik} > 0, i = 1, 2, ...), \tag{12}$$

where $\mu_{ik}$ are orthogonal coefficients that can be determined as in section 4.

**Theorem 7.** *Suppose that* $\{t_i\}_{i=1}^{\infty}$ *is dense in the interval* $[0,1]$*. If* $v(t) \in \Pi_3[0,1]$ *is a unique solution of Eq.* (11)*, then*

$$v(t) = \sum_{i=1}^{\infty}\sum_{k=1}^{i} \mu_{ik}\left[\widetilde{G}(t_k, v(t_k), Tv(t_k))\right]\bar{\psi}_i(t). \tag{13}$$

**Proof.** Let $v(t)$ be the solution of Eq. (11) that can be expanded in Fourier series. Since $\langle v(t), \varphi_i(t)\rangle_{\Pi_1} = v(t_i)$ and $\sum_{i=1}^{\infty}\langle v(t), \bar{\psi}_i(t)\rangle_{\Pi_3}\bar{\psi}_i(t)$ is convergent series for each $v(t) \in \Pi_3[0,1]$, then we have

$$\begin{aligned}
v(t) &= \sum_{i=1}^{\infty}\langle v(t), \bar{\psi}_i(t)\rangle_{\Pi_3}\bar{\psi}_i(t) = \sum_{i=1}^{\infty}\sum_{k=1}^{i}\mu_{ik}\langle v(t), \psi_k(t)\rangle_{\Pi_3}\bar{\psi}_i(t) \\
&= \sum_{i=1}^{\infty}\sum_{k=1}^{i}\mu_{ik}\langle v(t), \mathcal{D}^*\varphi_k(t)\rangle_{\Pi_3}\bar{\psi}_i(t) \\
&= \sum_{i=1}^{\infty}\sum_{k=1}^{i}\mu_{ik}\langle \mathcal{D}v(t), \varphi_k(t)\rangle_{\Pi_1}\bar{\psi}_i(t) \\
&= \sum_{i=1}^{\infty}\sum_{k=1}^{i}\mu_{ik}\left\langle \widetilde{G}(t, v(t), Tv(t)), \varphi_k(t)\right\rangle_{\Pi_1}\bar{\psi}_i(t) \\
&= \sum_{i=1}^{\infty}\sum_{k=1}^{i}\mu_{ik}\left[\widetilde{G}(t_k, v(t_k), Tv(t_k))\right]\bar{\psi}_i(t).
\end{aligned}$$

Therefore, the form of Eq. (13) is the exact solution of Eq. (11). The proof is complete. □

Since $\Pi_3[0,1]$ is a Hilbert space, the series

$$\sum_{i=1}^{\infty}\sum_{k=1}^{i}\mu_{ik}\left\langle \mathcal{D}v(t),\varphi_k(t)\right\rangle_{\Pi_1}\bar{\psi}_i(t)<\infty.$$

Hence, the truncated series

$$v_n(t)=\sum_{i=1}^{n}\sum_{k=1}^{i}\mu_{ik}\left[\widetilde{G}\left(t_k,v(t_k),Tv(t_k)\right)\right]\bar{\psi}_i(t) \tag{14}$$

is convergent in the sense of $\|\cdot\|_{\Pi_3[0,1]}$ and the numerical solution of Eq. (11) can be directly calculated by Eq. (14).

To analyze the most comprehensive computations, we mention that the solution depends on the internal structure of $\widetilde{G}$. That is, if $\widetilde{G}$ is linear, then the exact and the numerical solutions can be directly obtained by using Theorem 7. Whilst, if $\widetilde{G}$ is nonlinear, then the exact and the numerical solutions can be obtained iteratively by using the following process:

$$v(t)=\sum_{i=1}^{\infty}\Lambda_i\bar{\psi}_i(t),\ \Lambda_i=\sum_{k=1}^{i}\mu_{ik}\widetilde{G}\left(t_k,v(t_k),Tv(t_k)\right). \tag{15}$$

Let $t_1=0$, then $v(t_1)=0$. Set the initial function $v_0(t_1)=v(t_1)$, then $\widetilde{G}\left(t_1,v(t_1),Tv(t_1)\right)$ is known. Define the $n$-term numerical solution of $v(t)$ as follows:

$$v_n(t)=\sum_{i=1}^{n}\Lambda_i\bar{\psi}_i(t), \tag{16}$$

where $\Lambda_i=\sum_{k=1}^{i}\mu_{ik}\widetilde{G}\left(t_k,v_{n-1}(t_k),Tv_{n-1}(t_k)\right)$.

In the iterative process of Eq. (16), we can guarantee that the numerical solution $v_n$ satisfies the constraints conditions of Eq. (11).

## 4 Convergence of the RKHS method

In this section, we show that the $n$-term approximate solution $v_n(t)$ converges uniformly to exact solution $v(t)$ as $n\to\infty$ in the Hilbert space $\Pi_3[0,1]$.

**Theorem 8.** *If $\|v_{n-1}-v\|_{\Pi_3} arrow 0$, $t_n arrows$ $(narrow\infty)$, $\|v_n\|$ is bounded, and $\widetilde{G}(t,w_1,w_2)$ is continuous in $[0,1]$ with respect to $t,w_i$, $i=1,2$, then $\widetilde{G}(t_n,v_{n-1}(t_n),Tv_{n-1}(t_n)) arrow \widetilde{G}(s,v(s),Tv(s))$ as $narrow\infty$.*

**Proof.** By the reproducing property of $G_s(t)$, we have $v(t)=\langle v(\cdot),G_t(\cdot)\rangle_{\Pi_3}$ and $v'(t)=\langle v(\cdot),\partial_t G_t(\cdot)\rangle_{\Pi_3}$. From the continuity of $G_s(t)$ and and the Schwarz inequality, we get that $|v'(t)|=\left|\langle v(s),\partial_t G_t(s)\rangle_{\Pi_3}\right|\le\|v(s)\|_{\Pi_3}\|\partial_t G_t(s)\|_{\Pi_3}\le M_1\|v\|_{\Pi_3}$, $|v_{n-1}(s)-v(s)|=\left|\langle v_{n-1}(s)-v(s),G_t(s)\rangle_{\Pi_3}\right|$

$\leq \|v_{n-1}(s) - v(s)\|_{\Pi_3} \|G_t(s)\|_{\Pi_3} \leq M_2 \|v_{n-1} - v\|_{\Pi_3}$. From the last description as well, it follows that

$$\begin{aligned} |v_{n-1}(t_n) - v(s)| &= |v_{n-1}(t_n) - v_{n-1}(s) + v_{n-1}(s) - v(s)| \\ &\leq |v_{n-1}(t_n) - v_{n-1}(s)| + |v_{n-1}(s) - v(s)| \\ &\leq \left|(v_{n-1})'(\xi)\right| |t_n - s| + |v_{n-1}(s) - v(s)| \\ &\leq M_1 \|v\|_{\Pi_3} |t_n - s| + M_2 \|v_{n-1} - v\|_{\Pi_3}, \end{aligned}$$

where $\xi$ lies between $t_n$ and $s$. From the assumptions $\|v_{n-1} - v\|_{\Pi_3} \to 0$, $t_n \to s$ and the boundedness of $\|v_n\|$ as $n \to \infty$, it implies that $v_n(t_n) \to v(s)$ as $n \to \infty$. By the continuation of $\widetilde{G}$, we get the result directly. □

**Lemma 9.** *Suppose that* $\{t_i\}_{i=1}^{\infty}$ *is dense in the interval* $[0,1]$ *and* $v(t)$ *is the solution of Eq. (15), then* $\mathcal{D}v(t_k) = \mathcal{D}v_n(t_k)$ *as* $n \to \infty$.

**Proof.** Let $P_n$ be the projective operator such that $P_n{:}\Pi_3[0,1] \to \{\sum_{m=1}^{n} c_m \psi_m(t), c_m \in \mathbb{R}\}$.

Then, we have $\mathcal{D}v_n(t_k) = \langle v_n(\xi), \mathcal{D}_{t_k} G_{t_k}(\xi)\rangle_{\Pi_3} = \langle v_n(\xi), \psi_k(\xi)\rangle_{\Pi_3} = \langle P_n v(\xi), \psi_k(\xi)\rangle_{\Pi_3} = \langle v(\xi), P_n \psi_k(\xi)\rangle_{\Pi_3} = \langle v(\xi), \psi_k(\xi)\rangle_{\Pi_3} = \langle v(\xi), \mathcal{D}_{t_k} G_{t_k}(\xi)\rangle_{\Pi_3} = \mathcal{D}_{t_k}\langle v(\xi), G_{t_k}(\xi)\rangle_{\Pi_3} = \mathcal{D}v(t_k)$. □

**Theorem 10.** *Suppose that* $||v_n||_{\Pi_3}$ *is bounded in Eq.* (16) $\{t_i\}_{i=1}^{\infty}$ *is dense in the interval* $[0,1]$, *and Eq.* (11) *has a unique solution. Then, the n-term approximate solution* $v_n(t)$ *converges to the exact solution* $v(t)$ *of Eq.* (11) *and the exact solution is expressed as* $v(t) = \sum_{i=1}^{\infty} \Lambda_i \bar{\psi}_i(t)$, *where* $\Lambda_i$ *is given in the iterative formula* (16).

**Proof.** From the iterative formula (16), we have $v_n(t) = v_{n-1}(t) + \Lambda_n \bar{\psi}_n(t)$. Hence, $\|v_n(t)\|_{\Pi_3}^2 = \|v_{n-1}(t)\|_{\Pi_3}^2 + \Lambda_n^2$, which implies that $\|v_n(t)\|_{\Pi_3}^2 = \|v_0(t)\|_{\Pi_3}^2 + \sum_{i=1}^{n} \Lambda_i^2$. Since $\|v_n(t)\|_{\Pi_3}$ is bounded, monotone increasing and convergent as soon as $n \to \infty$, then there exists a positive constant $\beta$ such that $\sum_{i=1}^{n} \Lambda_i^2 = \beta$. For $m > n$, it follows that

$$\begin{aligned} \|v_m(t) - v_n(t)\|_{\Pi_3}^2 &= \|v_m - v_{m-1} + v_{m-1} - \ldots + v_{n+1} - v_n\|_{\Pi_3}^2 \\ &= \|v_m - v_{m-1}\|_{\Pi_3}^2 + \|v_{m-1} - v_{m-2}\|_{\Pi_3}^2 + \ldots + \|v_{n+1} - v_n\|_{\Pi_3}^2 \\ &= \sum_{l=n+1}^{m} \Lambda_l^2 \to 0, (m, n \to \infty), \end{aligned}$$

in view of $(v_m - v_{m-1}) \perp (v_{m-1} - v_{m-2}) \perp \ldots \perp (v_{n+1} - v_n)$. Considering the completeness of $\Pi_3[0,1]$, there exist $v(t) \in \Pi_3[0,1]$ such that $v_n(t) \to v(t)$ as soon as $n \to \infty$.

Again, from the iterative formula (16), we have $v(t) = \lim_{n\to\infty} v_n(t) = \sum_{i=1}^{\infty} \Lambda_i \bar{\psi}_i(t)$.

Thus, $\mathcal{D}v(t) = \sum_{i=1}^{\infty} \Lambda_i \mathcal{D}\bar{\psi}_i(t)$ and $\mathcal{D}v(t_k) = \sum_{i=1}^{\infty} \Lambda_i \left\langle \mathcal{D}\bar{\psi}_i(t), \varphi_k(t)\right\rangle_{\Pi_1} = \sum_{i=1}^{\infty} \Lambda_i \left\langle \bar{\psi}_i(t), \mathcal{D}^* \varphi_k(t)\right\rangle_{\Pi_3} = \sum_{i=1}^{\infty} \Lambda_i \left\langle \bar{\psi}_i(t), \psi_k(t)\right\rangle_{\Pi_3}$.

Consequently, $\sum_{k=1}^{i}\mu_{ik}\mathcal{D}v\left(t_k\right)=\sum_{k=1}^{i}\mu_{ik}\left(\sum_{i=1}^{\infty}\Lambda_i\left\langle\bar{\psi}_i\left(t\right),\psi_k\left(t\right)\right\rangle_{\Pi_3}\right)=\sum_{i=1}^{\infty}\Lambda_i\left\langle\bar{\psi}_i\left(t\right),\sum_{k=1}^{i}\mu_{ik}\psi_k\left(t\right)\right\rangle_{\Pi_3}=\sum_{i=1}^{\infty}\Lambda_i\left\langle\bar{\psi}_i\left(t\right),\bar{\psi}_k\left(t\right)\right\rangle_{\Pi_3}=\Lambda_k$. In view of Eq. (11), we have $\mathcal{D}v\left(t_k\right)=\widetilde{G}\left(t_k,v\left(t_k\right),Tv(t_k)\right)$. For the conduct of proceedings in the proof, since $\{t_i\}_{i=1}^{\infty}$ is dense in the interval $[0,1]$, there exists a subsequence $\left\{t_{n_j}\right\}_{j=1}^{\infty}$ such that $t_{n_j}\to s$ as $j\to\infty$. Observing that $\mathcal{D}v_{n_j}\left(t_{n_j}\right)=\widetilde{G}\left(t_{n_j},v_{n_j-1}\left(t_{n_j}\right),Tv_{n_j-1}(t_{n_j})\right)$, let $j\to\infty$, by the continuity of $\widetilde{G}$ and Theorem 8, we have $\mathcal{D}v\left(s\right)=\widetilde{G}\left(s,v\left(s\right),Tv(s)\right)$. Also, since $\bar{\psi}_i\left(t\right)\in\Pi_3\left[0,1\right]$, then $v\left(t\right)$ satisfies Eq. (11) and the constraints conditions. So, the proof of the theorem is complete. □

For the error behavior, if $\varepsilon_n=|v(t)-v_n(t)|$, where $v\left(t\right)$ and $v_n\left(t\right)$ are given in Eqs. (15) and (16), respectively. Then, one can write $\|\varepsilon_n\|_{\Pi_3}^2=\left\|\sum_{i=n+1}^{\infty}\Lambda_i\bar{\psi}_i\right\|_{\Pi_3}^2=\sum_{i=n+1}^{\infty}\left(\Lambda_i\right)^2$ and $\|\varepsilon_{n-1}\|_{\Pi_3}^2=\left\|\sum_{i=n}^{\infty}\Lambda_i\bar{\psi}_i\right\|_{\Pi_3}^2=\sum_{i=n}^{\infty}\left(\Lambda_i\right)^2$. Clearly, $\{\varepsilon_n\}_{n=1}^{\infty}$ is decreasing in the sense of $\|\cdot\|_{\Pi_3}$. Since $\sum_{i=1}^{\infty}\Lambda_i\bar{\psi}_i\left(t\right)$ is convergent series, then $\|\varepsilon_n\|_{\Pi_3}\to 0$ as $n\to\infty$.

## 5 Applications and numerical algorithm

To test the accuracy, simplicity and effectiveness of the RKHS algorithm, certain numerical examples with exact solutions are given. The results reveal that the method is highly accurate, rapidly converge, and convenient to handle various physical and engineering problems. Based on the algorithm, we pick $t_i=ih$, $i=1,2,...,6$, with step-size $h=0.16$ and take $n=26$, where $n$ is the number of terms of the Fourier series of the unknown function $u(t)$. The numerical computations are performed using Maple 13 software package. To allocating more, we present the following algorithm to summarize the procedure in finding the approximate solutions.

**Algorithm 11.** *To approximate the solution $u_n\left(t\right)$ of $u\left(t\right)$ for Eqs.* (1) *and* (2)*, do the following steps.*

**Step 1:** Fixed $t$ in $[0,1]$ and set $s\in[0,1]$;

If $s\le t$, let $G_s\left(t\right)=\sum_{i=1}^{6}a_i(s)t^{i-1}$;

else let $G_s\left(t\right)=\sum_{i=1}^{6}b_i(s)t^{i-1}$;

**Step 2:** Choose $n$ collocation points and do the following subroutine:

Set $t_i=\frac{i-1}{n-1}$, $i=1,2,...,n$;

Set $\psi_i(t)=\mathcal{D}_sG_s\left(t\right)|_{s=t_i}$;

**Step 3:** Obtain the orthogonalization coefficients $\mu_{i\rho}$ as follows

Let $c_{ik}=\left\langle\psi_i\left(t\right),\overline{\psi}_k\left(t\right)\right\rangle_{\Pi_3}$, and do the following subroutine:

For $i=1$, set $\mu_{11}=\|\psi_1\|_{\Pi_3}^{-1}$;

For $i=2,...,n$, set $\mu_{ii}=\left(\|\psi_i\|_{\Pi_3}^2-\sum_{k=1}^{i-1}c_{ik}^2\right)^{-0.5}$;

else (for $\rho<i$), set $\mu_{i\rho}=-\left(\sum_{k=\rho}^{i-1}c_{ik}\mu_{k\rho}\right)\left(\|\psi_i\|_{\Pi_3}^2-\sum_{k=1}^{i-1}c_{ik}^2\right)^{-0.5}$;

**Step 3:** For $i=1,2,...,n$, set

$\overline{\psi}_i(t)=\sum_{k=1}^{i}\mu_{ik}\psi_k(t)$;

**Step 4:** Set $t_1=0$, and choose an initial approximation $v_0(t_1)=v(t_1)$;

For $i=1$, set $\Lambda_1=\mu_{11}\widetilde{G}(0,v_0(0),Tv_0(0))$ and $v_1(t)=\Lambda_1\overline{\psi}_1$;

For $i=2,3,...,n$, set $\Lambda_i=\sum_{k=1}^{i}\mu_{ik}\widetilde{G}(t_k,v_{n-1}(t_k),Tv_{n-1}(t_k))$;

Set $v_n(t)=\sum_{i=1}^{n}\Lambda_i\bar{\psi}_i(t)$;

**Step 5:** Set $u_n(t)=v_n(t)+\gamma t$;

Solve a linear system $u_n(0)=0$ and $u_n(1)-\alpha u_n(\eta)=0$ to obtain $\gamma$.

Outcome: the numerical solution $u_n(t)$.

**Step 6:** Stop.

By applying Algorithm 1 throughout the numerical computations, we present some tabulate data, numerical comparison, and graphical results that discussed quantitatively at some selected grid points on $[0,1]$.

**Example 12.** Consider the singular linear differential equation.$u''(t)+\frac{1}{\sin(t)}u'(t)-\frac{1}{t(t-1)}u(t)-Tu(t)=f(t),$. with three-point boundary conditions$u(0)=0, u(1)-4u\left(\frac{1}{9}\right)=0$, where $Tu(t)=\int_0^1 t^2su(s)ds+\int_0^t(t+1)su(s)ds$, $0<s<t<1$ and $f(t)$ satisfies the existence and uniqueness of $u(t)$. Here, the singularities at the two endpoints $\{0,1\}$. However, the exact solution is $u(t)=t(t-1)\left(t-\frac{1}{9}\right)\cos(t)$.

The results of numerical analysis are approximate as much as is required within a logical error ratio that will be stored in a fixed number of digits. Using the RKHS algorithm, the comparison between exact and numerical solutions of Example 12 together with absolute and relative errors in $\Pi_3[0,1]$ are shown in Table 1. This is an indication of stability of the presented method.

Table 1. Numerical solutions and errors for Example 12.

| $t$ | Exact solution | Numerical solution | Absolute error | Relative error |
|---|---|---|---|---|
| 0.16 | −0.0064867414033 | −0.0064883615395 | $1.62014\times10^{-6}$ | $2.49761\times10^{-4}$ |
| 0.32 | −0.0431467576347 | −0.0431461185735 | $6.39061\times10^{-7}$ | $1.48113\times10^{-5}$ |
| 0.48 | −0.0816697618499 | −0.0816661092539 | $3.65260\times10^{-6}$ | $4.47240\times10^{-5}$ |
| 0.64 | −0.0977401806727 | −0.0977386264592 | $1.55421\times10^{-6}$ | $1.59015\times10^{-5}$ |
| 0.80 | −0.0767925617414 | −0.0767937406674 | $1.17893\times10^{-6}$ | $1.53521\times10^{-5}$ |
| 0.96 | −0.0186952221593 | −0.0186969923499 | $1.77019\times10^{-6}$ | $9.46868\times10^{-5}$ |

**Example 13.** Consider the singular nonlinear differential equation

$$u''(t) - \frac{1}{t^2(1-t)^2}u'(t) + \frac{1}{\sinh(t)}u(t) - u^2(t) - \sinh^{-1}(u(t)) - Tu(t) = f(t),$$

with three-point boundary conditions$u(0) = 0$, $u(1) - u\left(\frac{1}{2}\right) = 0$, where $Tu(t) = \int_0^1 tsu^3(s)\,ds + \int_0^t (t-s)u^2(s)\,ds$, $0 < s < t < 1$ and $f(t)$ satisfies the existence and uniqueness of $u(t)$. Here, the singularities at the two endpoints $\{0, 1\}$. However, the analytical solution is $u(t) = \left(t - \frac{1}{2}\right)^2 (t-1)^2 \sinh(t)$.

Using the RKHS algorithm, the comparison between exact and numerical solutions of Example 13 together with absolute and relative errors in $\Pi_3[0,1]$ are shown in Table 2.

Table 2. Numerical solutions and errors for Example 13.

| $t$ | Exact solution | Numerical solution | Absolute error | Relative error |
|---|---|---|---|---|
| 0.16 | 0.0131065322359 | 0.0131062996971 | $2.32539 \times 10^{-7}$ | $1.77422 \times 10^{-5}$ |
| 0.32 | 0.0048764035285 | 0.0048762184821 | $1.85046 \times 10^{-7}$ | $3.79473 \times 10^{-5}$ |
| 0.48 | 0.0000539334978 | 0.0000538664049 | $6.70929 \times 10^{-8}$ | $1.24399 \times 10^{-3}$ |
| 0.64 | 0.0017389788733 | 0.0017390244908 | $4.56175 \times 10^{-8}$ | $2.62324 \times 10^{-5}$ |
| 0.80 | 0.0031971815359 | 0.0031972745002 | $9.29643 \times 10^{-8}$ | $2.90770 \times 10^{-5}$ |
| 0.96 | 0.0003772918713 | 0.0003773895245 | $9.76532 \times 10^{-8}$ | $2.58827 \times 10^{-4}$ |

**Example 14.** Consider the singular nonlinear differential equation

$$u''(t) + \frac{1}{t(t-1)\left(t-\frac{1}{3}\right)}u'(t) + \frac{1}{(e^t-1)}u(t) - \cosh(u(t)) - Tu(t) = f(t),$$

with three-point boundary conditions$u(0) = 0$, $u(1) - 2u\left(\frac{1}{3}\right) = 0$, where $Tu(t) = \int_0^1 ts^2(8s-11)e^{-s\left(2s-\frac{1}{3}\right)}e^{u(s)}ds + \int_0^t \cosh(t)\,u^4(s)\,ds$, $0 < s < t < 1$ and $f(t)$ satisfies the existence and uniqueness of $u(t)$. Here, the singularities at multi-points $\{0, \frac{1}{3}, 1\}$ of the interval $[0,1]$. However, the analytical solution is $u(t) = t\left(t - \frac{1}{3}\right)\left(2t^2 - 3t + 1\right)$.

Using the RKHS algorithm, the comparison between exact and numerical solutions of Example 14 together with absolute and relative errors in $\Pi_3[0,1]$ are shown in Table 3.

Table 3. Numerical solutions and errors for Example 14.

| $t$ | Exact solution | Numerical solution | Absolute error | Relative error |
|---|---|---|---|---|
| 0.16 | −0.0158412800000 | −0.0158410408525 | $2.39147 \times 10^{-7}$ | $1.50965 \times 10^{-5}$ |
| 0.32 | −0.0010444799999 | −0.0010442321864 | $2.47814 \times 10^{-7}$ | $2.37260 \times 10^{-4}$ |
| 0.48 | 0.0014643200000 | 0.0014645926865 | $2.72686 \times 10^{-7}$ | $1.86221 \times 10^{-4}$ |
| 0.64 | −0.0197836799999 | −0.0197832643578 | $4.15642 \times 10^{-7}$ | $2.10093 \times 10^{-5}$ |
| 0.80 | −0.0448000000000 | −0.0447993897465 | $6.10253 \times 10^{-7}$ | $1.36217 \times 10^{-5}$ |
| 0.96 | −0.0221388799999 | −0.0221381979890 | $6.82011 \times 10^{-7}$ | $3.08060 \times 10^{-5}$ |

**Example 15.** Consider the singular nonlinear differential equation

$$u''(t) + \frac{1}{\ln(t+1)}u'(t) - \frac{1}{t\left(t-\frac{1}{4}\right)(t-1)}u(t) - u(t)\,e^{u(t)} - Tu(t) = f(x),$$

with three-point boundary conditions$u(0) = 0$, $u(1) - 3u\left(\frac{1}{4}\right) = 0$, where $Tu(t) = \int_0^1 (t-s)^2 e^{u(s)} ds + \int_0^t e^{s+t} e^{u(s)} ds$, $0 < s < t < 1$ and $f(t)$ satisfies the existence and uniqueness of $u(t)$. Here, the singularities at multipoints $\{0, \frac{1}{4}, 1\}$ of the interval $[0,1]$. However, the the analytical solution is $u(t) = \ln\left(t^2(1-t)\left(t - \frac{1}{4}\right) + 1\right)$.

Using the RKHS algorithm, the comparison between exact and numerical solutions of Example 15 together with absolute and relative errors in $\Pi_3[0,1]$ are shown in Table 4. It is clear from the tables that the numerical solutions are in close agreement with the exact solutions for all examples, while the accuracy is in advanced by using only few term of the RKHS iterations. The approximation values and the absolute errors of $u^{(i)}(t), i = 0, 1, 2$, at various $t$ in $[0,1]$ of Example 15 are graphically plotted in Figures 1, 2, and 3, respectively. Here, the numerical values for the exact solution approach smoothly to the $t$-axis by satisfying their boundary conditions. Indeed, decreasing the step-size increases the accuracy of the results while increasing the time required to simulate the problem.

Table 4. Numerical solutions and errors for Example 15.

| $t$ | Exact solution | Numerical solution | Absolute error | Relative error |
|---|---|---|---|---|
| 0.16 | −0.0019372352291 | −0.0019373982303 | $1.63001 \times 10^{-7}$ | $8.41412 \times 10^{-5}$ |
| 0.32 | 0.0048623993527 | 0.0048624655648 | $6.62121 \times 10^{-8}$ | $1.36172 \times 10^{-5}$ |
| 0.48 | 0.0271830114104 | 0.0271831781099 | $1.66700 \times 10^{-7}$ | $6.13249 \times 10^{-6}$ |
| 0.64 | 0.0559150456224 | 0.0559153019544 | $2.56332 \times 10^{-7}$ | $4.58431 \times 10^{-6}$ |
| 0.80 | 0.0680324103918 | 0.0680327200535 | $3.09662 \times 10^{-7}$ | $4.55168 \times 10^{-6}$ |
| 0.96 | 0.0258367772964 | 0.0258368978659 | $1.20569 \times 10^{-7}$ | $4.66658 \times 10^{-6}$ |

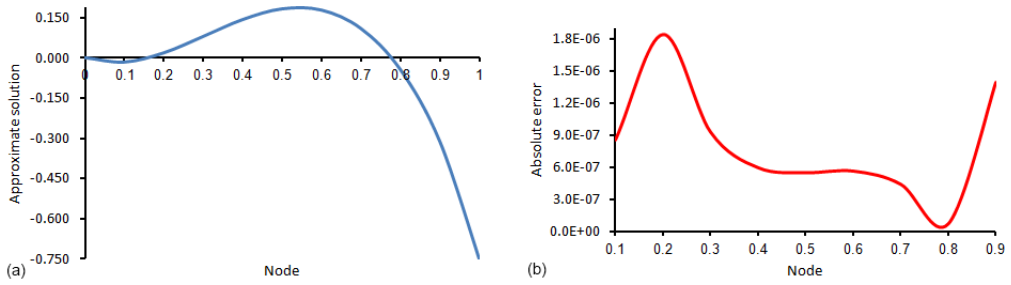


Figure 1: Graphical results of $u(x)$ of Example 15: (a) approximate solution (b) absolute error.

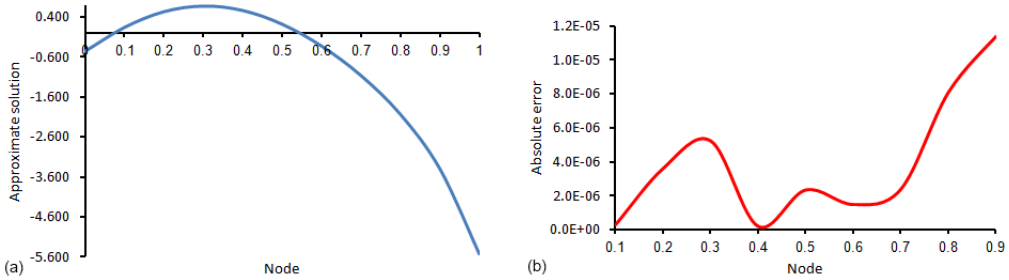


Figure 2: Graphical results of $u'(x)$ of Example 15: (a) approximate solution (b) absolute error.

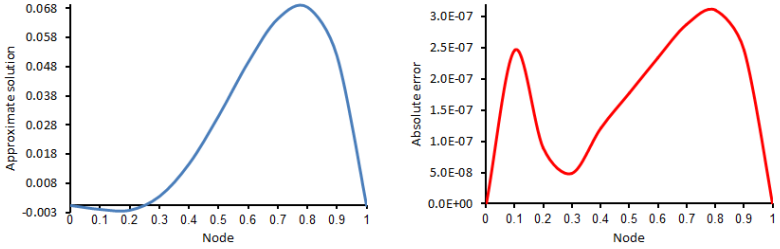


Figure 3: Graphical results of $u''(t)$ of Example 15: (a) solution solution, (b) absolute error.

## 6 Concluding remarks

This article is presented in the RKHS algorithm as a novel solver for a class of singular BVPs restricted by Fredholm-Volterra operators. This algorithm and its conjugate operator are employed to construct the complete orthonormal basis in the reproducing kernel space $\Pi_3[0,1]$. As well, it is applied in a direct way without using linearization, perturbation, or any restrictive assumptions. we can conclude that the RKHS algorithm is very powerful and efficient tool in finding analytical-numerical solutions for a wide class of such models arising in sciences and engineering. Besides, for numerical experiments, higher accuracy can be achieved in computing further RKHS iterations. Thus, the RKHS algorithm is capable of reducing the volume of the computational work and complexity while still maintaining the high accuracy of the numerical results.

## References

[1] Y. Sun, *Positive solutions of singular third-order three-point boundary value problem*, Journal of Mathematical Analysis and Applications, 306 (2005), 589–603.

[2] X. Du, Z. Zhao, *Existence and uniqueness of smooth positive solutions to a class of singular m-point boundary value problems*, Boundary Value Problems, 2009 (2009), Article ID 191627, 1-13.

[3] J. Liu, H. Feng, X. Feng, *Multiplicity of positive solutions for a singular second-order three-point boundary value problem with a parameter*, Journal of Applied Mathematics, 2014 (2014), Article ID 603203, 1-8.

[4] P. Singh, *A second-order singular three-point boundary value problem*, Applied Mathematics Letters, 17 (2004), 969-976.

[5] H.B. Thompson, C. Tisdell, *Three-point boundary value problems for second-order, ordinary, differential equations,* Mathematical and Computer Modelling, 34 (2001), 311-318.

[6] F. Geng, *Solving singular second order three-point boundary value problems using reproducing kernel Hilbert space method,* Applied Mathematics and Computation, 215 (2009), 2095-2102.

[7] Y. Zhou, Y. Xu, *Positive solutions of three-point boundary value problems for systems of nonlinear second order ordinary differential equations*, Journal of Mathematical Analysis and Applications, 320 (2006) 578-590.

[8] I. Komashynska, M. Al-Smadi, O. Abu Arqub, S. Momani, *An efficient analytical method for solving singular initial value problems of nonlinear systems*, Applied Mathematics and Information Sciences, 10 (2016), 647-656.

[9] O. Abu Arqub, M. Al-Smadi, *Numerical algorithm for solving time-fractional partial integrodifferential equations subject to initial and Dirichlet boundary conditions. NumericalMethods for Partial Differential Equations,* 2017.

[10] M. Al-Smadi, O. Abu Arqub, N. Shawagfeh, S. Momani, *Numerical investigations for systems of second-order periodic boundary value problems using reproducing kernel method*, Applied Mathematics and Computation, 291 (2016), 137-148.

[11] O. Abu Arqub, M. Al-Smadi, *Numerical algorithm for solving two-point, second-order periodic boundary value problems for mixed integro-differential equations*, Applied Mathematics and Computation, 243 (2014), 911-922.

[12] F. Geng, M. Cui, *Solving singular nonlinear second-order periodic boundary value problems in the reproducing kernel space*, Applied Mathematics and Computation, 192 (2007), 389-398.

[13] H.L. Weinert, *Reproducing Kernel Hilbert Spaces: Applications in Statistical Signal Processing*, Hutchinson Ross, 1982.

[14] A. Berlinet, C.T. Agnan, *Reproducing Kernel Hilbert Space in Probability and Statistics*, Kluwer Academic Publishers, Boston, Mass, USA, 2004.

[15] A. Daniel, *Reproducing Kernel Spaces and Applications*, Springer, Basel, Switzerland, 2003.

[16] M. Cui, Y. Lin, *Nonlinear Numerical Analysis in the Reproducing Kernel Space*, Nova Science, New York, NY, USA, 2009.

[17] M. Al-Smadi, O. Abu Arqub, S. Momani, *A computational method for two-point boundary value problems of fourth-order mixed integrodifferential equations*, Mathematical Problems in Engineering, Vol. 2013 (2013), Article ID 832074, 1-10.

[18] O. Abu Arqub, M. Al-Smadi, N. Shawagfeh, *Solving Fredholm integro-differential equations using reproducing kernel Hilbert space method*, Applied Mathematics and Computation, 219 (2013), 8938-8948.

[19] O. Abu Arqub, M. Al-Smadi, S. Momani, T. Hayat, *Application of reproducing kernel algorithm for solving second-order, two-point fuzzy boundary value problems*, Soft Computing, 21 (23), 7191-7206, 2017.

[20] F. Geng, M. Cui, *A reproducing kernel method for solving nonlocal fractional boundary value problems*, Applied Mathematics Letters, 25 (2012), 818-823.

[21] Z. Altawallbeh, M. Al-Smadi, R. Abu-Gdairi, *Approximate solution of second-order integrodifferential equation of Volterra type in RKHS method*, Int. Journal of Math. Analysis, 7 (44), (2013) 2145-2160.

[22] G. Gumah, K. Moaddy, M. Al-Smadi, I. Hashim. *Solutions of uncertain Volterra integral equations by fitted reproducing kernel Hilbert space method*, Journal of Function Spaces, 2016 (2016), Article ID 2920463, 1-11.

[23] K. Moaddy, M. Al-Smadi, O. Abu Arqub, I. Hashim, *Analytic-numeric treatment for handling system of second-order, three-point BVPs*, AIP Conference Proceedings, Vol. 1830, 020025, 2017.

[24] S. Momani, O. Abu Arqub, A. Freihat, M. Al-Smadi, *Analytical approximations for Fokker-Planck equations of fractional order in multistep schemes*, Applied and Computational Mathematics, 15 (2016), 319-330.

[25] M. Al-Smadi, A. Freihat, M. Abu Hammad, S. Momani, O. Abu Arqub, *Analytical approximations of partial differential equations of fractional order with multistep approach*, Journal of Computational and Theoretical Nanoscience 13 (2016), 7793-7801.

[26] M. Al-Smadi, A. Freihat, H. Khalil, S. Momani, R.A. Khan, *Numerical multistep approach for solving fractional partial differential equations*, Int J Comput Methods, 14 (2017),1–15.

[27] M. Al-Smadi, A. Freihat, O. Abu Arqub, N. Shawagfeh, *A Novel Multistep Generalized Differential Transform Method for Solving Fractional-order Lü Chaotic and Hyperchaotic Systems*, Journal of Computational Analysis and Applications, 19 (2015), 713-724.

[28] K. Moaddy, A. Freihat, M. Al-Smadi, E. Abuteen, I. Hashim, *Numerical investigation for handling fractional-order Rabinovich-Fabrikant model using the multistep approach*, Soft Computing, 2016 (2016), 1-10.

[29] A. El-Ajou, O. Abu Arqub, M. Al-Smadi, *A general form of the generalized Taylor's formula with some applications*, Applied Mathematics and Computation, 256 (2015), 851-859.

[30] H. Khalil, R.A. Khan, M. Al-Smadi, A. Freihat, *Approximation of solution of time fractional order three-dimensional heat conduction problems with Jacobi Polynomials*, Punjab University Journal of Mathematics, 47 (2015), 35-56.